American Mineralogist, Volume 81, pages 800–810, 1996

Time evolution of pericline twin domains in alkali feldspars: A computer-simulation study

I. Tsatskis* and E.K.H. Salje

Department of Earth Sciences, University of Cambridge, Downing Street, Cambridge CB2 3EQ, U.K.

Abstract

A large-scale computer simulation of Al-Si ordering and the corresponding development of a twin microstructure in alkali feldspars is reported for the first time. In the simulation, the order-disorder transition is driven by long-range, strain-mediated interactions between ordering atoms. These interactions are the result of an elastic accommodation of two tetrahedra of different sizes, AlO_4 and SiO_4, in the feldspar framework structure. The elementary step in changing the Al-Si distribution in this model is the interchange of two Al and Si atoms occupying neighboring corner-sharing tetrahedra. A combined Monte Carlo–lattice-relaxation method was used. An initially homogeneous disordered sample was "annealed" at a temperature, T, below the transition. The mesoscopic microstructure at $T < T_c$ is dominated by the spontaneous strain of the triclinic structure. The formation and subsequent coarsening of the pericline twins as developed in a thin slab parallel to the {010} plane was observed; the orientations of twin domain boundaries deviate significantly on a local scale from the macroscopic direction predicted by the compatibility condition.

Introduction

Crystals undergoing phase transitions very often exhibit complicated domain patterns below the transition temperature because of the degeneracy of the low-symmetry phase and the local character of the transformation. A simple example of such degeneracy is the easy-axis ferromagnet in which spontaneous magnetization can be oriented, for example, up or down. In the case of ferroelastic phase transitions, in which the spontaneous strain appears below the transition temperature, there exist several orientational variants of the low-temperature phase. The phase transitions in alkali feldspars considered in this paper are order-disorder transitions accompanied by large spontaneous strain. In such transitions the deformation of a crystal is the consequence of ordering; the elastic strain energy may account for about 50% of the total excess Gibbs free energy (Salje et al. 1985a). The process of ordering is local, and in some part of the crystal any orientational variant can occur with the same probability. As a result of such orientational variants, the crystal in the low-symmetry phase may consist of domains of all possible orientational variants separated by twin boundaries.

In this paper we focus on the development of the twin microstructure and the corresponding transient patterns. The direct observation of Al-Si ordering in alkali feldspars is hindered by the sluggish kinetics of the exchange process (e.g., Putnis and McConnell 1980). However, such kinetic processes can be easily simulated by computer modeling. The results of such simulation can then be compared with direct transmission electron microscopy (TEM) observations of partially ordered alkali feldspars. It is the main aim of this paper to present such simulated microstructures, some of which may appear counterintuitive. We believe, however, that such microstructures may be present in natural samples, and we hope that our results will stimulate subsequent TEM studies. Preliminary results have recently been briefly discussed (Tsatskis and Salje 1995).

This study is concerned with the time evolution of microstructures using the Monte Carlo method. The quantity "time" is defined in such methods in terms of the number of attempts to change the atomic configuration (e.g., Kehr and Binder 1987). The assessment of the correlation between this internal time scale and true, natural time is not trivial, however. In this paper we use only the internal time (i.e., the Monte Carlo time). It might be useful for the reader to equate this time, t_{MC}, in an approximate manner with the natural time, t, by

$$t = t_{MC}\exp(E_a/kT) \quad (1)$$

where E_a is the activation energy of the ordering process.

The text is organized in the following way. In the remaining part of this section the framework structure, the order-disorder phase transition, and the twin microstructure below the transition in alkali feldspars are briefly reviewed. The general model for the numerical simulation of the microstructure and its application to feldspars are described in the next section. The computer modeling itself and related problems, including the important issue of the efficient calculation of the energy difference between two successive configurations of ordering Al and Si atoms, are the focus of the third section. The last section is a description of the results of the simulation and their discussion.

* Former name: I. Masanskii.

0003–004X/96/0708–0800$05.00

The crystal structure of alkali feldspars (chemical formula MT_4O_8, M = K, Na; T = Al, Si; $T_4 = AlSi_3$) is a three-dimensional framework of corner-sharing TO_4 tetrahedra, with M atoms serving as spacers and occupying large framework cavities. The basic structural unit of this framework is a four-tetrahedron ring in which alternate pairs of vertices point in opposite directions; such rings form crankshaft-like chains running parallel to the a axis. An AlO_4 tetrahedron is somewhat larger in comparison with an SiO_4 tetrahedron; the ratio of mean Al-O and Si-O bond lengths is about 1.08 (e.g., Putnis 1992). The tetrahedra are relatively rigid, and the difference in size between the two types of tetrahedra is accommodated within the framework by changes in their relative positions without loss of the topology of the framework. K and Na spacers also differ in size, contributing thereby to the deformation of the framework. Details of the structural properties of alkali feldspars have been previously described in great detail (Smith and Brown 1988; Ribbe 1994; Brown and Parsons 1994).

At sufficiently high temperatures the Al and Si atoms at T1 and T2 sites in the alkali feldspars are in a disordered state. The sites T1 and T2 are topologically distinct, so that some degree of order (described by the order parameter Q_t) is maintained at all temperatures; i.e., the T1-T2 disordering is nonconvergent (Smith and Brown 1988; Harrison and Salje 1994; Carpenter and Salje 1994). The order-disorder transition with the order parameter Q_{od} relates to ordering of Al and Si on the T1o and T1m sites (Salje 1985; Salje et al. 1985a). The order parameter Q_{od} couples bilinearly with the spontaneous strain with the components e_4 and e_6.

In the triclinic phase ($Q_{od} \neq 0$), a characteristic twin microstructure is observed in alkali feldspars (e.g., Eggleton and Buseck 1980; Fitz Gerald and McLaren 1982; McLaren 1984; Krause et al. 1986; Brown and Parsons 1994). Permissible orientations of twin boundaries can be determined from the requirement that the atomic displacements in the domain-wall plane are identical for both adjacent domains. This requirement is expressed mathematically as the compatibility condition (Sapriel 1975):

$$\sum_{ij} (e_{ij} - e'_{ij}) x_i x_j = 0 \qquad (2)$$

where e_{ij} and e'_{ij} denote components of spontaneous strain tensors for two domains, and x_i is the coordinate of a point in the domain-boundary plane. In the case under consideration the tensors of the spontaneous strain have the form

$$e = -e' = \begin{pmatrix} 0 & e_{xy} & 0 \\ e_{xy} & 0 & e_{yz} \\ 0 & e_{yz} & 0 \end{pmatrix} = \begin{pmatrix} 0 & e_6 & 0 \\ e_6 & 0 & e_4 \\ 0 & e_4 & 0 \end{pmatrix} \qquad (3)$$

and Equation 2 has two solutions (Salje et al. 1985b): the albite twin law

$$y = 0 \qquad (4)$$

and the pericline twin law

$$z = -(e_{xy}/e_{yz})x = -(e_6/e_4)x. \qquad (5)$$

The albite twin law (Eq. 4) defines a {010} domain wall; the pericline twin law (Eq. 5) corresponds to the domain boundary orthogonal to the {010} plane, with an orientation that depends on the ratio of the components e_4 and e_6 of the spontaneous strain tensor. In the case of potassium feldspar, for example, the pericline twin walls are nearly perpendicular to the {001} plane.

The model for the microstructure formation

In this section the model used for the simulation of the microstructure development is formulated in general terms, and then its application to alkali feldspars is described.

The underlying physical picture is an order-disorder phase transition that generates spontaneous strain. The ordering atoms of types A and B (here Al and Si) occupy certain sets of positions in a perfect crystalline structure or host matrix. The phase transition is, as usual, the result of interaction between the ordering atoms. It is assumed that the ordering atoms interact only elastically (through the host matrix), i.e., indirectly, and that direct chemical (short-range) and Coulombic interactions can be neglected (Heine 1994, personal communication). The origin of the elastic interatomic interaction is the static distortion of the host matrix by the ordering atoms. In the absence of the ordering atoms the host matrix is an ideal crystal, and all its atoms are in mechanical equilibrium (we do not consider here the vibrations of the host atoms). When the ordering atoms are inserted into the host matrix, each ordering atom produces external stress with respect to the host matrix shifting its atoms away from the initial equilibrium positions. As a result, internal forces arise in the host matrix that tend to return the host atoms to the initial positions. A new state of equilibrium corresponding to a given distribution of ordering atoms is then reached in which the sum of external and internal forces acting on each atom of the host matrix vanishes. In this new equilibrium state the host atoms are displaced from the initial positions, and the host matrix is distorted. Different configurations of ordering atoms correspond to different sets of displacements. In the simplest possible approximation the resulting displacement of a host atom is a superposition of displacements caused by individual ordering atoms. If we now consider two ordering atoms in the otherwise empty host matrix, it is clear that one atom "feels" the distortion of the host matrix created by another atom, and this results in the effective long-range elastic interaction between these two atoms.

More formally, if a system consists of two subsystems that are not independent, i.e., the subsystems interact with each other, then the Hamiltonian of this system, generally speaking, should be a sum of three contributions. The first two terms are the Hamiltonians of the isolated subsystems, and the third term represents the interaction between these subsystems. In our case the crystal consists

of the ordering atoms and the host matrix. Therefore, the Hamiltonian under consideration has the form

$$H = H_{\text{host}} + H_{\text{ord}} + H_{\text{int}} \tag{6}$$

where H_{host} and H_{ord} are Hamiltonians of the host matrix and the ordering atoms, respectively, and H_{int} is the interaction Hamiltonian. We now specify the form of all three Hamiltonians. The Hamiltonian of the host matrix, which is its potential energy, is a function of the static displacements $\mathbf{u}$ of host atoms and describes the energy increase when the host matrix is pulled out of the mechanical equilibrium; the latter corresponds to the energy minimum. In the case of sufficiently small displacements it is possible to expand the host-matrix energy in powers of the displacements and to retain only the first nonzero (quadratic) term. This is the harmonic approximation usually used in the theory of lattice dynamics (e.g., Ashcroft and Mermin 1976). The zero-order term, which does not depend on displacements, is ignored. Further, because it is supposed that the ordering atoms do not interact directly, their energy is configurationally independent, and the second contribution to the Hamiltonian (Eq. 6) H_{ord} is zero. Finally, the interaction Hamiltonian describes the effect of forces $\mathbf{f}$ with which an ordering atom acts on neighboring host atoms. We assume that these forces have constant values, regardless of the positions of the host atoms; this means that the interaction term is the linear function of displacements, because of the relation

$$f^i_n = -\frac{\partial H_{\text{int}}}{\partial u^i_n} \tag{7}$$

where f^i_n is the ith Cartesian component of a force acting on the atom at site n of the host matrix, and u^i_n is the corresponding displacement. Obviously, an ordering atom of each kind has its own set of forces, and the resulting force on the host matrix is therefore a function of the configuration of the ordering atoms. A particular configuration of the ordering atoms is fully described by the set of occupation numbers p^α_l, α = A, B,

$$p^\alpha_l = \begin{cases} 1, & \text{atom of type } \alpha \text{ at site } l \\ 0, & \text{otherwise} \end{cases} \tag{8}$$

and l is the position of an ordering atom. The force f^i_n (Eq. 7) depends on the occupation numbers for the ordering atoms surrounding the atom at site n of the host matrix and can be conveniently written in their terms as

$$f^i_n = \sum_l \left(F^{i\text{A}}_{nl} p^{\text{A}}_l + F^{i\text{B}}_{nl} p^{\text{B}}_l\right) = \sum_{l\alpha} F^{i\alpha}_{nl} p^\alpha_l. \tag{9}$$

In this equation $F^{i\alpha}_{nl}$ is the ith Cartesian component of the so-called Kanzaki force (Khachaturyan 1983) with which the ordering atom of type α at site l acts on the host atom at site n. Taking into account Equations 7 and 9, we finally get the full Hamiltonian of the system in the following form:

$$H = \tfrac{1}{2} uAu - uFp = \tfrac{1}{2} \sum_{nm} \sum_{ij} u^i_n A^{ij}_{nm} u^j_m - \sum_{nl} \sum_i \sum_\alpha u^i_n F^{i\alpha}_{nl} p^\alpha_l \tag{10}$$

where A is the Born–von Kármán tensor of the host matrix. It is seen that in the Hamiltonian (Eq. 10) the variables corresponding to the two subsystems (displacements of the host atoms and occupation numbers of the ordering atoms) are coupled bilinearly because of the interaction term H_{int}. The result (Eq. 10) can also be obtained by representing the internal energy of the host matrix as a series in powers of the small displacements of the host atoms and disregarding third-order and higher terms (Krivoglaz 1969; Khachaturyan 1983). Similar Hamiltonians have been used to study transient tweed and twin patterns that arise in the process of ordering on simple lattices caused by elastic interactions (Marais et al. 1991; Salje and Parlinski 1991; Salje 1992; Parlinski et al. 1993a, 1993b; Bratkovsky et al. 1994a, 1994b, 1994c). Unlike in the case of the harmonic approximation for the host matrix, here the first-order contribution is nonzero because of applied external forces. The actual positions of the ordering atoms are not specified in the model; the Hamiltonian (Eq. 10) contains only the displacements of the host atoms. In fact, this Hamiltonian describes the host matrix subjected to external forces, and these forces depend on a particular configuration of the ordering atoms, which is described in terms of the occupation numbers.

Let us turn now to the quantitative description of the effective long-range interaction between the ordering atoms starting from the Hamiltonian (Eq. 10). To find static displacements corresponding to a given configuration of the ordering atoms, it is necessary to minimize the energy of the system [i.e., the Hamiltonian (Eq. 10)] with respect to displacements $\mathbf{u}_n$ for a given set of the occupation numbers representing this configuration. The static displacements $\mathbf{u}^{\text{st}}$ are, therefore, solutions of the coupled equations

$$\frac{\partial H}{\partial u^i_n} = (Au - Fp)^i_n = \sum_m \sum_j A^{ij}_{nm} u^j_m - \sum_l \sum_\alpha F^{i\alpha}_{nl} p^\alpha_l = 0 \tag{11}$$

and can be written as

$$(\mathbf{u}^{\text{st}})^i_n = (A^{-1}Fp)^i_n = \sum_{ml} \sum_j \sum_\alpha (A^{-1})^{ij}_{nm} F^{j\alpha}_{ml} p^\alpha_l. \tag{12}$$

Decomposing an instantaneous displacement of the host atom into two parts,

$$\mathbf{u}_n = \mathbf{u}^{\text{st}}_n + \Delta\mathbf{u}_n, \tag{13}$$

substituting this sum into the initial Hamiltonian (Eq. 10), and using Equation 12, we arrive at the following expression:

$$H = \tfrac{1}{2}pVp + \tfrac{1}{2}\Delta u A \Delta u$$
$$= \tfrac{1}{2}\sum_{kl}\sum_{\alpha\beta} p_l^\alpha V_{lk}^{\alpha\beta} p_k^\beta + \tfrac{1}{2}\sum_{nm}\sum_{ij} \Delta u_n^i A_{nm}^{ij} \Delta u_m^j. \quad (14)$$

The first term is the standard Hamiltonian used in the phenomenological theory of ordering (de Fontaine 1979; Ducastelle 1991), which contains only variables corresponding to the ordering atoms (i.e., occupation numbers), whereas the second term describes harmonic vibrations of the host atoms around new (displaced due to static external forces) equilibrium positions. The Born–von Kármán tensor A and, therefore, the phonon frequencies are the same as in the case of the undistorted host matrix; in the harmonic approximation static deformations do not affect lattice vibrations. In this Hamiltonian the degrees of freedom corresponding to the two subsystems are completely separated, and at finite temperatures the thermal vibrations of the host atoms are independent of the configuration of the ordering atoms. The effective interaction V between the ordering atoms in Equation 14 has the form

$$V_{lk}^{\alpha\beta} = -(F^{\mathrm{T}} A^{-1} F)_{lk}^{\alpha\beta} = -\sum_{nm}\sum_{ij} (F^{\mathrm{T}})_{ln}^{\alpha i} (A^{-1})_{nm}^{ij} F_{mk}^{j\beta}. \quad (15)$$

Using spin variables s_i,

$$p_i^{\mathrm{A}} = \tfrac{1}{2}(1 + s_i), \qquad p_i^{\mathrm{B}} = \tfrac{1}{2}(1 - s_i) \quad (16)$$

it is easy to show that the effective Hamiltonian for ordering in the grand canonical ensemble,

$$\tilde{H} = \tfrac{1}{2}pVp - \sum_{\alpha} \mu^\alpha N^\alpha \quad (17)$$

where μ^α and N^α are the chemical potential and total number of atoms of type α, respectively, is formally equivalent to that of the Ising model (de Fontaine 1979; Ducastelle 1991),

$$\tilde{H} = -\tfrac{1}{2}\sum_{lk} J_{lk} s_l s_k - \sum_l h_l s_l \quad (18)$$

where the effective exchange integral J_{lk} and the magnetic field h_l are given by

$$J_{lk} = \tfrac{1}{4}(2V_{lk}^{\mathrm{AB}} - V_{lk}^{\mathrm{AA}} - V_{lk}^{\mathrm{BB}}) \quad (19)$$

$$h_l = \tfrac{1}{2}(\mu^{\mathrm{A}} - \mu^{\mathrm{B}}) - \tfrac{1}{4}\sum_k (V_{lk}^{\mathrm{AA}} - V_{lk}^{\mathrm{BB}}). \quad (20)$$

Inserting Expression 15 for the effective interaction between the ordering atoms into Equation 19 yields

$$J_{lk} = \tfrac{1}{4}[(F^{\mathrm{A}} - F^{\mathrm{B}})^{\mathrm{T}} A^{-1} (F^{\mathrm{A}} - F^{\mathrm{B}})]_{lk}$$
$$= \tfrac{1}{4}\sum_{nm}\sum_{ij} (F^{\mathrm{A}} - F^{\mathrm{B}})_{ln}^{i} (A^{-1})_{nm}^{ij} (F^{\mathrm{A}} - F^{\mathrm{B}})_{mk}^{j}. \quad (21)$$

This equation shows that it is the difference $F^{\mathrm{A}} - F^{\mathrm{B}}$ between the Kanzaki forces for the two types of ordering atoms which matters, and not the values of F^{A} and F^{B}. It is important to note that the site-diagonal matrix elements $V_{ll}^{\alpha\beta}$ and J_{ll} of the effective interatomic interaction V and exchange integral J have nonzero values; in other words, there exists the effect of a self-interaction of the ordering atoms. The reason for the self-interaction is easy to understand: A single ordering atom placed into the empty host matrix distorts the latter and thereby changes the energy of the system. This energy change corresponds precisely to the diagonal matrix element of the effective interaction V. This self-interaction is important in the discussion that follows of the calculation of the energy difference corresponding to the interchange of a pair of atoms. It can be shown that in reciprocal space the effective spin interaction (Eq. 21) has the singularity at the point $\mathbf{k} = 0$ (e.g., de Fontaine 1979), similar to the singularity of the velocity of sound (Folk et al. 1976; Cowley 1976). This singularity is characteristic of the elastic interactions: The $\mathbf{k} \to 0$ limit of the Fourier transform of the effective interaction depends on the direction along which the point $\mathbf{k} = 0$ is approached.

Applying the model described above to alkali feldspars, we consider the host matrix as a regular network of interconnected ideal O tetrahedra of the same size, with the connection topology characteristic of feldspars. The alkali atoms play the role of structural spacers. In other words, we attribute K, Na, and O atoms to the host matrix. The host matrix has monoclinic symmetry. The difference in size between K and Na spacers is not very important for this study and is ignored. In a further study, however, one might want to analyze the effect of Al-Si ordering on K-Na exsolution using a similar model. Here we substitute K and Na by the same atom of average size. The structure is to some extent idealized for computational reasons, in the sense that the bases of all tetrahedra in a horizontal four-tetrahedron ring lie in the {010} plane, and two of four tetrahedra are pointed strictly upwards and two strictly downwards; i.e., in this structural model no buckling of the rings occurs (Fig. 1). This idealization results, in particular, in the value $\beta = 120°$, whereas the experimental value is $\beta = 116°$ (Megaw 1973; Kroll and Ribbe 1987). Al and Si atoms are tetrahedrally coordinated by O and constitute, according to our classification, the ordering atoms. Starting to specify the model, we define the Kanzaki forces with which these two kinds of atoms act on the host matrix. Application of the external forces to the host matrix should lead to the difference in average sizes of the AlO_4 and SiO_4 tetrahedra. Consider first an isolated O tetrahedron. We define its size according to the SiO_4 tetrahedron, i.e., the presence of an Si atom inside does not produce any distortion of the tetrahedron, and the corresponding Kanzaki forces are zero. The Al atom inside the tetrahedron results in the homogeneous expansion of the tetrahedron with no change in its shape. To achieve this effect, the Kanzaki forces applied to the O atoms at the tetrahedron vertices are directed outward along the lines connecting Al and O atoms. No other forces exerted on the host matrix by the ordering atoms are taken into account, which means that the only sources of deformation of the K-Na-O host matrix are Al atoms distributed over the centers of the O

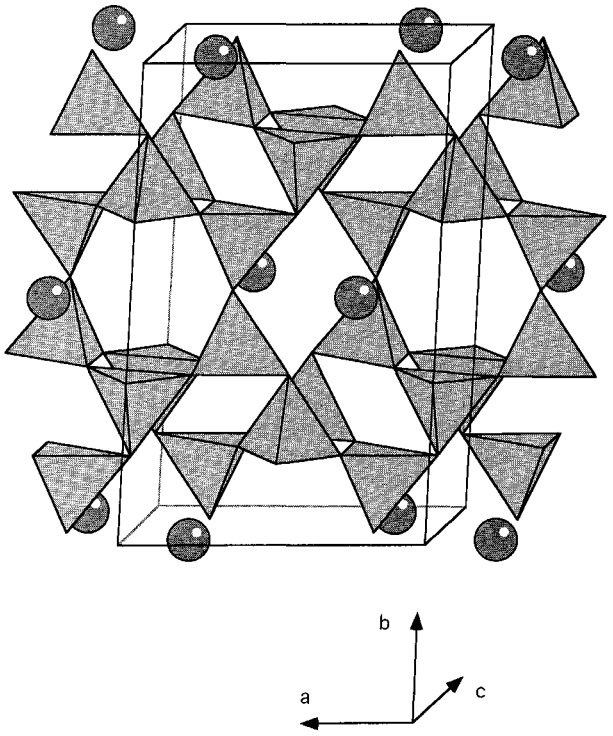

FIGURE 1. The unit cell of the simulated thin slab of alkali feldspar-like structure defined with respect to the whole slab. The simulated sample is obtained by the translation of the cell in a and c directions. All tetrahedra are of the same size and correspond to the host lattice before applying the Kanzaki forces. Spheres represent alkali atoms.

tetrahedra. They increase the volume of the corresponding tetrahedra, and the host matrix accommodates the resulting stresses.

The next step is to select the necessary interatomic bonds in the host matrix, i.e., to define nonzero matrix elements of the Born–von Kármán tensor A (Eq. 10). We imagine the host matrix as consisting of balls (the host atoms) and harmonic springs connecting these balls. We can distinguish several sets of springs. Springs belonging to the first set connect each two O atoms in an individual tetrahedron and provide the elastic resistance of the tetrahedron to the Kanzaki forces produced by the Al atom. The TO_4 tetrahedra are relatively rigid structural units in the framework, and the spring constants of the intratetrahedron O-O bonds are considerably greater than those of other bonds. The second set of springs relates to M-O and M-M bonds. These bonds are responsible for the stability of the framework and prevent structural collapse around the alkali positions. In our model of the host matrix there are (per M atom) three M-O springs in the mirror plane connecting the M atom with the two O_A atoms, eight M-O springs between the M atom and its O neighbors, O_A (1), O_B, O_C, and O_D, which are off the mirror plane and above and below it, and three M-M springs in the mirror plane. Finally, we add some of the O-O

TABLE 1. Spring constants for different groups of springs in the host matrix

Spring	Spring constant
Intratetrahedron O-O	100
Intratetrahedron O-O (surface tetrahedra)	110
Intertetrahedra O-O	50
M-O and M-M	10

bonds that connect, in addition to the common O atom, two neighboring tetrahedra. The role of these intertetrahedral links is to enhance the strain-mediated repulsion between two Al atoms occupying the corner-sharing tetrahedra and to stabilize the T-O-T bond angle. To achieve the latter, additional bond-bending terms explicitly dependent on the angle value are sometimes introduced into the Hamiltonian (Sanders et al. 1984). We do not intend to fit parameters of the model to experimental properties of alkali feldspars, like elastic moduli, spontaneous strain in the low-temperature phase, etc. Instead, our strategy is to use the smallest parameter set possible, provided that the correct ordered phase and reasonable directions of the pericline domain walls are obtained. Following this approach, only four spring constants are used, two for the intratetrahedral and intertetrahedral O-O bonds and one for M-O and M-M bonds. The fourth spring constant is for the intratetrahedral O-O bonds in {010} surface tetrahedra; the reason for this choice is discussed at the end of the next section. The numerical values of the spring constants are listed in Table 1.

Before we discuss details of the computer simulation, let us briefly return to the analytical approach outlined above. Strictly speaking, the ball-and-spring model for the host matrix used in the simulations is not exactly identical with the model described by the harmonic Hamiltonian H_{host}. The difference is the anharmonicity of the ball-and-spring Hamiltonian, which appears simply for geometrical reasons and has nothing to do with any anharmonicity of interatomic springs. However, for small displacements these anharmonic effects become negligibly small, and the two models give the same results.

THE COMPUTER SIMULATION AND THE ENERGY-DIFFERENCE PROBLEM

In the present work the kinetics of ordering is studied using the Monte Carlo–lattice-relaxation method (Marais et al. 1991; Bratkovsky et al. 1994a, 1994b, 1994c). The elementary microscopic process that leads to the evolution of the state of order in a binary mixture is usually assumed to be an interchange of two, not very distant (in many cases nearest-neighbor only) A and B atoms, the so-called Kawasaki spin-exchange dynamics. According to the Metropolis "importance sampling" algorithm (see, e.g., Binder and Stauffer 1987), this interchange takes place with a transition probability that is a function of the energy difference

$$\Delta E = E_f - E_i \quad (22)$$

where E_i and E_f are the energies of the configurations of the ordering atoms before and after the interchange (initial and final configurations), respectively. To perform the computer simulation at reasonable CPU times, it is necessary to develop an efficient method of calculating the energy difference (Eq. 22) between initial and final configurations.

As was already discussed in the previous section, the evolution in time of the system described by the Hamiltonian (Eq. 10) can be decomposed into two processes: atomic ordering accompanied by the static distortion of the host matrix and harmonic vibrations of the host atoms around the positions determined by this distortion. The characteristic time scales of these two processes are very different, so that we can average over the fast (phonon) degrees of freedom. It is difficult, if at all possible, to calculate the interaction (Eq. 15 or 21) analytically or numerically, especially in the case of structures with complicated unit cells, because such a calculation would mean an inversion of a very large ($3N \times 3N$, where N is the number of the host atoms in a simulated sample), sparse matrix A. There exists, however, another approach to this problem: One can rewrite the configurational part of the Hamiltonian (Eq. 14) using Equation 12 for the static displacements

$$H = \tfrac{1}{2}pVp = \tfrac{1}{2}\mathbf{u}^{st}A\mathbf{u}^{st} - \mathbf{u}^{st}Fp. \quad (23)$$

This equation shows that instead of calculating the effective interatomic interaction, V, it is possible to calculate numerically the static distortion (relaxation) of the host matrix corresponding to a particular configuration of the ordering atoms and then to compute the energy of this configuration according to Equation 23. This procedure is adopted in the simulation described here.

Two methods of calculating the host-matrix relaxation are implemented in the computer code. The first method is a numerical solution of the equation describing the motion of an individual classical particle (a host atom in the present case) under the influence of external forces and a fictitious force of friction,

$$m\mathrm{d}^2\mathbf{u}/\mathrm{d}t^2 + \gamma\,\mathrm{d}\mathbf{u}/\mathrm{d}t = \mathbf{f} \quad (24)$$

where m is the atomic mass, t is time, γ is friction coefficient, and $\mathbf{f}$ is the external force. This equation is solved using molecular dynamics. The second method uses the equation corresponding to the purely relaxational dynamics,

$$\mathrm{d}\mathbf{u}/\mathrm{d}t = \mathbf{f} \quad (25)$$

and the Euler method is used for its numerical solution (Press et al. 1986). The external force $\mathbf{f}$ in Equations 24 and 25 is the sum of the Kanzaki force F and the reaction force of the deformed host matrix. The solutions of these two equations tend to the static displacement $\mathbf{u}^{st}$ as $t \to \infty$.

The calculation of the static distortion of the host matrix described here, and even more so our Monte Carlo simulation, can be reasonably effective only when using highly parallel computer architecture. We now mention briefly some details concerning software and hardware involved in the simulation. The simulation was performed using the massively parallel computer AMT DAP 610 (AMT and DAP standing for "active memory technology" and "distributed array of processors," respectively) located at the Department of Applied Mathematics and Theoretical Physics, University of Cambridge. The AMT DAP 610 is a square 64×64 matrix of elementary processors served by a host workstation. Each elementary processor operates on its own data according to a common instruction stream that is broadcast from a central processor. This hardware architecture and the high-level language FORTRAN-PLUS make it possible to process in parallel entire vectors and matrices. It is the natural choice for simulating a sample that consists of $n_1 \times n_2 \times n_3$ unit cells, where $n_1 = n_2 = 64$. In the case of such sample an individual elementary processor stores the information about n_3 unit cells. The number of unit cells in the third direction (n_3) is arbitrary but restricted by such factors as the calculation speed and the degree of complexity of the unit cell. As a rule, the typical values of n_3 acceptable from this point of view are considerably smaller than 64 even for simple lattices, and the simulated sample unavoidably has the shape of a slab.

We now consider in detail the problem of calculating the energy difference (Eq. 22) between the initial and final configurations, which enters the Monte Carlo transition probability and is the central quantity to be calculated in the process of the simulation. Every elementary Monte Carlo step (the interchange of two nearest-neighbor atoms in the case of the Kawasaki dynamics) involves, in principle, two relaxations of the host matrix, one for each of the two configurations. This is unsatisfactory because the calculation of the lattice relaxation is very time-consuming and, in addition, we lose the important possibility of interchanging atoms belonging to different pairs using parallel procedure. In terms of the degree of parallelization and the calculation speed, the acceptable solution would be to have one host-matrix relaxation per simultaneous attempts to exchange atoms in each pair belonging to some chosen set of nonoverlapping pairs of ordering atoms covering the whole simulated sample. Surprisingly enough, this is possible. Let us consider, along with the interchange of atoms of some selected pair described above, another procedure that is the exchange of these two atoms in the field of fixed host matrix relaxed before with respect to the initial configuration. We refer to the corresponding energy differences associated with these two procedures for the pair of atoms at sites k and l as ΔE_{kl} and $\Delta\tilde{E}_{kl}$, respectively. It can be shown that these two energy differences are connected by a relation

$$\Delta E_{kl} = \Delta\tilde{E}_{kl} + 4J_{kl} - 2J_{kk} - 2J_u \quad (26)$$

where J_{kl} is defined by Equation 19. In the case considered in this paper the Kanzaki forces corresponding to

TABLE 2. The contents of the computational unit cell defined with respect to the whole slab

Species	Number
Host O atoms	34
Host M atoms	6
Ordering T atoms	16
Springs	193
Kanzaki forces	64
Kawasaki pairs	30

one species of atoms, say of B type, are equal to zero. According to Equations 15 and 19, this means that

$$V^{AA} = -4J,\ V^{AB} = V^{BB} = 0. \tag{27}$$

In this case the combination of the interactions entering Equation 26 and constituting the difference between the correct and incorrect energy differences can be expressed in terms of the energy E_k^A of a single A atom in the otherwise empty host matrix,

$$E_k^A = \tfrac{1}{2}V_{kk}^{AA} \tag{28}$$

and the similar energy E_{kl}^{AA} for a pair of A atoms,

$$E_{kl}^{AA} = V_{kl}^{AA} + \tfrac{1}{2}V_{kk}^{AA} + \tfrac{1}{2}V_{ll}^{AA}. \tag{29}$$

Finding the corresponding interactions from Equations 27–29 and inserting them into Equation 26 we finally have

$$\Delta E_{kl} = \Delta\tilde{E}_{kl} + \delta E_{kl} \tag{30}$$

$$\delta E_{kl} = 2E_k^A + 2E_l^A - E_{kl}^{AA}. \tag{31}$$

Equations 30 and 31 mean that the energies (Eqs. 28 and 29) and, therefore, the difference δE_{kl} between ΔE_{kl} and $\Delta\tilde{E}_{kl}$ can be calculated prior to the simulation and subsequently used for the calculation of the correct energy difference. The correction δE_{kl} is quite easy to calculate because for an infinite sample it is the same for all unit cells and depends only on sublattice indices. In the case of the finite sample used in the simulation this correction has noticeable spatial dependence, especially very close to the sample boundaries. In the simulation presented in this paper we ignored this spatial variation and calculated δE_{kl} for one of the unit cells in the center of the sample. Having reduced the calculation of ΔE_{kl} to that of $\Delta\tilde{E}_{kl}$, we can process in parallel as many nonoverlapping pairs

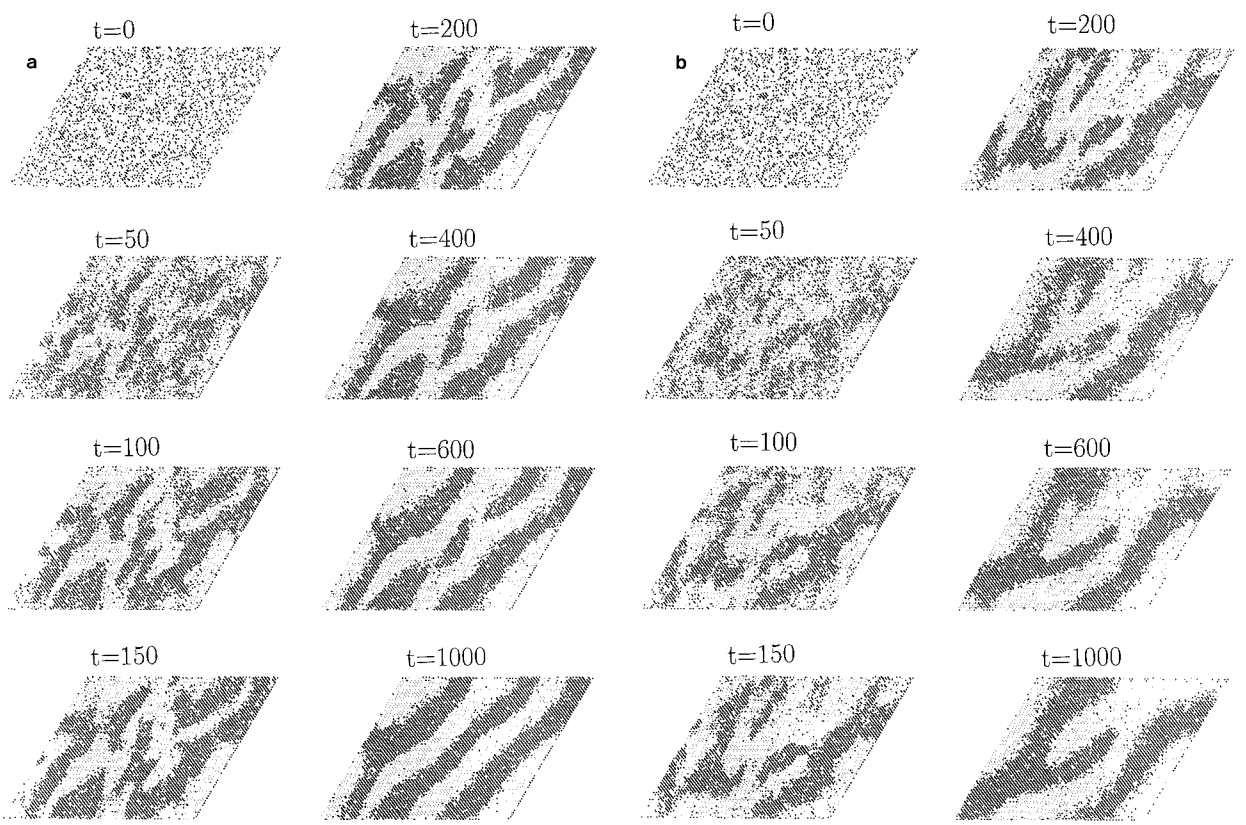

FIGURE 2 (above and right). Sequences of snapshots of the simulated twin microstructure corresponding to different annealing times, t (indicated in Monte Carlo steps per ordering atom). Only Al atoms distributed over T1 positions of a single crankshaft are shown. Different symbols (heavy and light dots) are used to distinguish between T1o and T1m sites. The first snapshot in each sequence corresponds to the initial, totally disordered Al-Si distribution. The annealing temperature increases from **a** to **c**; the approximate values of the T/T_c ratio are 0.3 (**a**), 0.5 (**b**), and 0.7 (**c**).

of ordering atoms as necessary. The Monte Carlo step consists then of the following substeps: (1) relaxing the host matrix according to initial configuration; (2) choosing a set of nonoverlapping pairs of ordering atoms; (3) calculating $\Delta\tilde{E}$ for each pair; (4) calculating ΔE using Equations 30 and 31; (5) making a Monte Carlo decision concerning the interchange of atoms of each pair according to the transition probability.

We now discuss briefly some remaining points important for the simulation. First, in the case of the ferroelastic phase transition described by a Hamiltonian that is a function of atomic displacements, the use of periodic boundary conditions is questionable because the spontaneous strain appears below the transition temperature and leads to a macroscopic deformation of the sample. For example, a monodomain sample in the ferroelastic phase is homogeneously deformed; the spontaneous strain tensor is constant throughout its volume. The displacement vector is therefore a linear function of atomic coordinates, which is incompatible with the periodic boundary conditions. Two other types of boundary conditions, free and clamped (see, for example, the discussion in Heine et al. 1994), are possible in this case. In our simulation we always used the free boundary conditions. Second, the formal stability analysis of the host matrix (all phonon frequencies must be positive for the crystal structure to be stable) is not performed; however, any instability is easily noticed and can be eliminated by taking into account additional interatomic bonds. In particular, we found that the bonds between spacers (K, Na) are important for the mechanical stability of the structure. The addition and removal of springs is straightforward because the computer code is quite flexible: As far as the host matrix is concerned, it uses only a topology of interatomic bonds in a unit cell of a crystal and allows it to simulate arbitrary lattices. Third, for actual simulation we used the ball-and-spring model for the host matrix, which, as against the harmonic Hamiltonian H_{host}, is, strictly speaking, anharmonic. However, the degree of anharmonicity is small; its magnitude was controlled during the simulation by monitoring the deviations from the relation

$$E_{\text{tot}} = -E_{\text{host}} = \tfrac{1}{2}E_{\text{int}} \tag{32}$$

where E_{tot}, E_{host}, and E_{int} are the energies corresponding to the Hamiltonians H, H_{host}, and H_{int}, respectively, in Equation 6 in the case $\mathbf{u} = \mathbf{u}^{\text{st}}$. This relation holds for the harmonic model (Eq. 10) and can be derived from Equations 10 and 12.

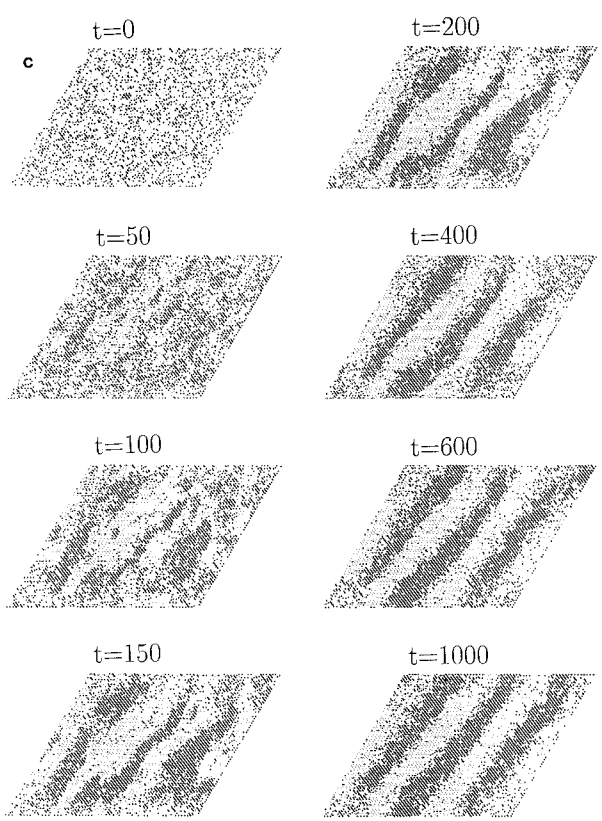

In the case of alkali feldspars the unit cell is quite complicated: It contains four formula units, i.e., 52 atoms. As a result, the simulated sample has the form of a very thin slab (or film); the computational unit cell defined for the whole slab (Fig. 1) contains slightly more than four formula units (56 atoms; see Table 2). In our simulation the slab has {010} orientation, which allows the observation of only the pericline twins; the simulated slab contains two crankshafts in the b direction (Fig. 1). The presence of the {010} free surfaces in the sample, with surface-to-volume ratio close to unity (the thin-slab geometry), creates additional problems. In the case of a crystal with a free surface undergoing the order-disorder phase transition the distribution of the ordering atoms becomes a function of the distance from the surface. Generally, the closer the atomic layer is to the surface, the more significant is the deviation of all crystal properties, in particular, concentrations of different kinds of atoms, from the bulk values. In the feldspar structure considered here, it is energetically favorable for the Al atoms to gather at the {010} surfaces of the simulated slab because it is easier for the slab to accommodate large AlO_4 tetrahedra at the surface rather than in the bulk (in our model there are no Coulombic interactions that maintain local charge neutrality). To avoid this effect and mimic the properties of bulk alkali-feldspar crystal, we slightly increased the strengths of the intratetrahedron bonds at the {010} surfaces. The criterion is the natural requirement of equality of the energies of a single Al atom at the surface and in the crystallographically equivalent layer inside the slab. This leads to a 10% increase in the spring constants of the surface intratetrahedron bonds (see Table 1).

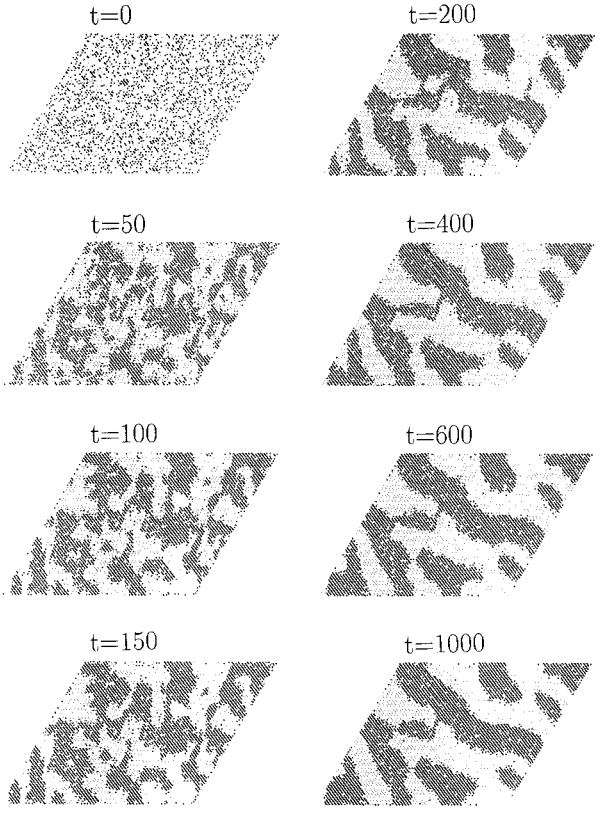

FIGURE 3. The same sequence of snapshots as in Figure 2 but for a different set of the host-matrix parameters.

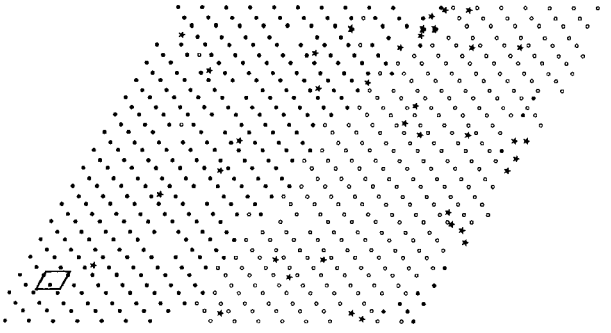

FIGURE 4. Magnified view of the area in one of the snapshots of Figure 2a (t = 1000) containing a solitary domain wall. Solid and open circles show T1o and T1m sites, respectively. In addition, stars mark Al atoms at T2 sites. A {010} projection of the unit cell (Fig. 1) is also shown.

RESULTS AND DISCUSSION

All simulations of the kinetics of microstructure formation described in this paper started from an initially disordered sample. More precisely, the simulations always started from a completely random Al-Si distribution, which is the hypothetical equilibrium configuration at infinite temperature. The sample was then instantly cooled across the transition temperature to a temperature at which the disordered phase is unstable, and then it was annealed at this temperature.

Sequences of snapshots of the twin microstructure in the simulated sample annealed at various temperatures, T, below the transition are shown in Figure 2. The values of the ratio T/T_c are approximate because it was difficult to determine the transition temperature accurately; the transition was smeared out because of finite-size effects. Only Al atoms belonging to a single crankshaft and located at T1 sites are shown in Figure 2, and different symbols are used to represent Al atoms at T1o and T1m sites. The Al atoms at T2 positions and all Si and host atoms are not shown in order to clearly distinguish the two variants of the ordered phase. At early stages of the ordering kinetics very fast local ordering and formation of the pericline twin domains were found. At the beginning, ordering and coarsening occurred simultaneously, and no clear distinction between these two processes was possible; after a short time, however, the local ordering was almost complete, and the pattern consisted of a fine mixture of well-defined regions in which the order parameter Q_{od} acquires positive or negative values. At early stages of annealing it was very difficult, and sometimes impossible (see, in particular, Fig. 3 discussed below), to observe the preferential orientation of the domain boundaries. The patches of the ordered phase continued to coarsen at later stages, and the preferential orientation of the domain walls gradually appeared. At even later stages, the system arranged itself into a pattern of relatively wide stripes of pericline twins aligned mainly along the direction described by the pericline twin law (Eq. 5) at a macroscopic level. The evolution of the sample at this stage was very slow, making it problematic to monitor further development of the stripe pattern. However, even in this regime the domain walls experienced significant deviations from the soft direction at a local scale. As the temperature increased and approached the transition point, the transitional areas between pericline twins became more and more diffuse. This is in complete agreement with the predictions of the continuum Landau-Ginzburg theory, according to which the width of a domain wall increases with temperature and finally diverges at the instability point (e.g., Salje 1993). The same sequence of snapshots for a slightly different set of the host-matrix parameters is shown in Figure 3. The preferential orientation for the domain boundaries is now quite different from what we observed in Figure 2. This change of orientation is not surprising because the soft direction of the pericline domain walls is sensitive to the ratio of the two nonzero components of the spontaneous strain tensor, as can be seen from Equation 5, which depends in turn on the choice of model parameters. Finally, the magnified picture of the configuration of Al atoms in the area containing a single domain wall is shown in Figure 4. It illustrates the internal structure of the pericline domain boundaries obtained in the simulation. In this case

the Al atoms at T2 sites are also indicated using different symbols, so that the distribution of all Al atoms is shown. Note that in some snapshots maximum deviations from the soft direction and noticeably higher degrees of disorder occur close to the slab edges. These deviations may be a consequence of the finite-size effects, ignoring the spatial variation of the correction δE_{kl} to the energy difference (Eq. 30), or both. The obvious consistent approach to the elimination of the second possibility is to calculate the above energy correction for the sufficient number of unit cells, including those at the edges of the sample, and to interpolate this function subsequently. This procedure will be implemented in future simulations.

The main results of the simulation can be summarized as follows. The pericline wall has only one symmetry constraint, namely, it must contain the crystallographic b axis. Its actual orientation depends on the ratio e_6/e_4 of the components of the spontaneous strain, i.e., the wall can rotate around the b axis as the ratio e_6/e_4 changes. When the crystal is quenched through T_c, the Al and Si atoms order locally and build up local strain. The twin walls accommodate this local strain, so that their orientation corresponds to the lattice deformation on a length scale of a few unit cells. This lattice deformation deviates substantially from that of the uniformly ordered sample. Local segments of walls at the early stages are not well aligned, therefore. With increasing degree of order, the spontaneous strain becomes more uniform, and a global alignment of walls is observed.

The second main result of the simulation is that pericline walls are not smooth on an atomistic scale. In the simulation we found that the wall thickness at temperatures well below the transition temperature is always ~1–2 unit cells, i.e., approximately 10–15 Å. This result seems to support the idea that there is a minimum thickness for a pericline wall when the temperature approaches absolute zero. The origin of this minimum thickness appears to be geometrical in nature, namely, that an atomistically perfect pericline wall cannot be constructed along an arbitrary direction containing the crystallographic b axis. The orientation of the wall is determined by the macroscopic compatibility condition (Eq. 2), which contains no direct information about the underlying crystal structure. Only under exceptional circumstances do such walls coincide with crystallographic planes that are apt to form structural twin planes. Generally, the orientation of the twin walls does not correlate with the crystal structure, leading to faceting of the wall. This faceting is then the reason for the effective finite thickness of the twin wall.

The third result concerns the kinetic process of the Al-Si ordering. In our simulation two processes can be identified. The first process leads to local ordering and the formation of a fine kinetic microstructure. The second process involves the coarsening of the stripe structure as a result of the rearrangement of locally ordered patches. There are no direct experimental observations related to laboratory experiments that could be compared to our results. Transient tweed microstructures have been found in Al-Si disordering experiments in sodium feldspar, however (Wruck et al. 1991). The tweed structures look very similar to our simulated microstructures, bearing in mind that the actual planes of observations are different in the two cases. No such microstructures were found for T1-T2 (dis)ordering in sanidine (Salje and Kroll 1990). To explore further the intriguing similarity between the transient microstructures for T1o-T1m ordering and disordering we plan to perform computer simulations of the disordering process.

Our ultimate goal is the simulation of ordering and microstructure in bulk samples of minerals on a mesoscopic length scale. To approach this goal, the modeling of larger and, in particular, thicker samples is necessary. An efficient enough computer code and, as a consequence, sufficiently high simulation speed are also necessary. Our computer code provided the simulation speed of about 200 Monte Carlo steps per ordering atom per hour in the simulation described here. In principle, this speed should allow us to simulate up to 10–20 crankshafts in future work.

References cited

Ashcroft, N.W., and Mermin, N.D. (1976) Solid state physics, 826 p. Saunders College, Philadelphia, Pennsylvania.

Binder, K., and Stauffer, D. (1987) A simple introduction to Monte Carlo simulation and some specialized topics. In K. Binder, Ed., Applications of the Monte Carlo method in statistical physics, p. 1–36. Springer, Berlin.

Bratkovsky, A.M., Salje, E.K.H., Marais, S.C., and Heine, V. (1994a) Theory and computer simulation of tweed texture. Phase Transitions, 48, 1–13.

Bratkovsky, A.M., Salje, E.K.H., and Heine, V. (1994b) Overview of the origin of tweed texture. Phase Transitions, 52, 77–84.

Bratkovsky, A.M., Marais, S.C., Heine,V., and Salje, E.K.H. (1994c) The theory of fluctuations and texture embryos in structural phase transitions mediated by strain. Journal of Physics: Condensed Matter, 6, 3679–3696.

Brown, W.L., and Parsons, I. (1994) Feldspars in igneous rocks. In I. Parsons, Ed., Feldspars and their reactions, p. 449–499. Kluwer, Dordrecht, the Netherlands.

Carpenter, M.A., and Salje, E.K.H. (1994) Thermodynamics of nonconvergent cation ordering in minerals: III. Order parameter coupling in potassium feldspar. American Mineralogist, 79, 1084–1098.

Cowley, R.A. (1976) Acoustic phonon instabilities and structural phase transitions. Physical Review B, 13, 4877–4885.

de Fontaine, D. (1979) Configurational thermodynamics of solid solutions. Solid State Physics, 34, 73–274.

Ducastelle, F. (1991) Order and phase stability in alloys, 511 p. North-Holland, Amsterdam.

Eggleton, R.A., and Buseck, P.R. (1980) The orthoclase-microcline inversion: A high-resolution transmission electron microscope study and strain analysis. Contributions to Mineralogy and Petrology, 74, 123–133.

Fitz Gerald, J.D., and McLaren, A.C. (1982) The microstructures of microcline from some granitic rocks and pegmatites. Contributions to Mineralogy and Petrology, 80, 219–229.

Folk, R., Iro, H., and Schwabl, F. (1976) Critical statics of elastic phase transitions. Zeitschrift für Physik B, 25, 69–81.

Harrison, R.H., and Salje, E.K.H. (1994) X-ray diffraction study of the displacive phase transition in anorthoclase, grain-size effects and surface relaxations. Physics and Chemistry of Minerals, 21, 325–329.

Heine, V., Bratkovsky, A.M., and Salje, E.K.H. (1994) The effect of clamped and free boundaries on long range strain coupling in structural phase transitions. Phase Transitions, 52, 85–93.

Kehr, K.W., and Binder, K. (1987) Simulation of diffusion in lattice gases and related kinetic phenomena. In K. Binder, Ed., Applications of the Monte Carlo Method in Statistical Physics, p. 181–221. Springer, Berlin.

Khachaturyan, A.G. (1983) Theory of structural transformations in solids, 574 p. Wiley, New York.

Krause, C., Kroll, H., Breit, U., Schmiemann, I., and Bambauer, H.-U. (1986) Formation of low-microcline twinning in tweed-orthoclase and its Al, Si order estimated by ALCHEMI and X-ray powder methods. Zeitschrift für Kristallographie, 174, 123–124.

Krivoglaz, M.A. (1969) Theory of X-ray and thermal neutron scattering by real crystals, 405 p. Plenum, New York.

Kroll, H., and Ribbe, P. H. (1987) Determining (Al,Si) distribution and strain in alkali feldspars using lattice parameters and diffraction-peak positions: A review. American Mineralogist, 72, 491–506.

Marais, S.C., Heine, V., Nex, C.M.M., and Salje, E.K.H. (1991) Phenomena due to strain coupling in phase transitions. Physical Review Letters, 66, 2480–2483.

McLaren, A.C. (1984) Transmission electron microscope investigations of the microstructures of microclines. NATO ASI, C137, 373–409.

Megaw, H.D. (1973) Crystal structures: A working approach, 563 p. Saunders, Philadelphia, Pennsylvania.

Parlinski, K., Salje, E.K.H., and Heine, V. (1993a) Annealing of tweed microstructure in high-T_c superconductors studied by a computer simulation. Acta metallurgica et materialia, 41, 839–847.

Parlinski, K., Heine, V., and Salje, E.K.H. (1993b) Origin of tweed texture in the simulation of a cuprate superconductor. Journal of Physics: Condensed Matter, 5, 497–518.

Press, W.H., Flannery, B.P., Teukolsky, S.A., and Vetterling, W.T. (1986) Numerical recipes: The art of scientific computing, 818 p. Cambridge University Press, Cambridge.

Putnis, A. (1992) Introduction to mineral sciences, 457 p. Cambridge University Press, Cambridge.

Putnis, A., and McConnell, J.D.C. (1980) Principles of mineral behaviour, 257 p. Blackwell Scientific, Oxford, U.K.

Ribbe, P.H. (1994) The crystal structures of the aluminium-silicate feldspars. In I. Parsons, Ed., Feldspars and their reactions, p. 1–49. Kluwer, Dordrecht, the Netherlands.

Salje, E.K.H. (1985) Thermodynamics of sodium feldspar: I. Order parameter treatment and strain induced coupling effects. Physics and Chemistry of Minerals, 12, 93–98.

——— (1992) Application of Landau theory for the analysis of phase transitions in minerals. Physics Reports, 215, 49–99.

——— (1993) Phase transitions in ferroelastic and co-elastic crystals, 276 p. Cambridge University Press, Cambridge.

Salje, E., Kuscholke, B., Wruck, B., and Kroll, H. (1985a). Thermodynamics of sodium feldspar: II. Experimental results and numerical calculations. Physics and Chemistry of Minerals, 12, 99–107.

Salje, E., Kuscholke, B., and Wruck, B. (1985b) Domain wall formation in minerals: I. Theory of twin boundary shapes in Na-feldspar. Physics and Chemistry of Minerals, 12, 132–140.

Salje, E.K.H., and Kroll, H. (1990) Kinetic rate laws derived from order parameter theory: III. Al-Si ordering in sanidine. Physics and Chemistry of Minerals, 17, 563–568.

Salje, E.K.H. and Parlinski, K. (1991) Microstructures in the high-T_c superconductors. Superconductor Science and Technology, 4, 93–97.

Sanders, M.J., Leslie, M., and Catlow, C.R.A. (1984). Interatomic potentials for SiO_2. Journal of the Chemical Society: Chemical Communications, 1271–1273.

Sapriel, J. (1975) Domain-wall orientations in ferroelastics. Physical Review B, 12, 5128–5140.

Smith, J.V., and Brown, W.L. (1988) Feldspar minerals, vol. 1, 828 p. Springer, Berlin.

Tsatskis, I., and Salje, E.K.H. (1995) Computer simulation of a microstructure in a potassium feldspar. Mineralogical Magazine, 59, 623–628.

Wruck, B., Salje, E., and Graeme-Barber, A. (1991) Kinetic rate laws derived from order parameter theory: IV. Kinetics of Al-Si disordering in Na-feldspars. Physics and Chemistry of Minerals, 17, 700–710.

Manuscript received June 16, 1995
Manuscript accepted February 26, 1996